Enhanced Proton Exchange Membrane Fuel Cell Parameter Estimation Using Birds of Prey-Based Optimization

Lotfi GAFSAOUI[1], Ahmed JERIDI[2] and Abderrahmen ZAAFOURI[3]

Abstract— **Accurate parameter identification is essential for developing reliable proton exchange membrane fuel cell (PEMFC) models, since their voltage–current characteristics are highly nonlinear and strongly affected by empirical and semi-empirical parameters. This paper proposes a BPBO-based parameter estimation approach for PEMFC models using the Birds of Prey-Based Optimization algorithm. The identification problem is formulated as a constrained optimization task in which the sum of squared errors (SSE) between experimental and simulated stack voltages is minimized. The proposed method is validated using two benchmark PEMFC stacks, namely the BCS 500 W and NedStack PS6 systems. The obtained results show that BPBO provides accurate parameter estimates and achieves a close agreement between measured and simulated polarization curves. Comparative and statistical analyses further confirm the competitive accuracy, robustness, and convergence behavior of BPBO with respect to several well-established optimization algorithms.**

Index Terms— **roton exchange membrane fuel cell, PEMFC, Birds of Prey-Based Optimization, BPBO, parameter identification, metaheuristic optimization, BCS 500 W, NedStack PS6roton exchange membrane fuel cell, PEMFC, Birds of Prey-Based Optimization, BPBO, parameter identification, metaheuristic optimization, BCS 500 W, NedStack PS6P**

I. Introduction

Proton exchange membrane fuel cells (PEMFCs) have attracted considerable attention as efficient and clean energy conversion devices due to their high power density, low operating temperature, fast start-up capability, and low pollutant emissions [1], [2]. In PEMFC systems, electrical energy is produced through the electrochemical reaction between hydrogen supplied to the anode and oxygen supplied to the cathode [5]. Accurate PEMFC modeling is therefore essential for system design, performance prediction, optimization, diagnosis, and control under varying operating conditions [17].

PEMFC modeling approaches can generally be classified into empirical, physics-based, and hybrid models. Empirical models are derived from experimental data obtained under specific operating conditions, whereas physics-based models describe the electrochemical, thermodynamic, and transport phenomena occurring inside the cell. Hybrid models combine physical equations with empirical or semi-empirical parameters in order to improve both accuracy and practical applicability [2], [6], [20]. However, PEMFC voltage–current behavior remains highly nonlinear and strongly affected by temperature, pressure, humidity, reactant flow rates, and internal voltage losses. As a result, accurate identification of the model parameters remains a challenging constrained optimization problem [18], [21], [26].

Parameter estimation using experimental polarization data is a key step for calibrating PEMFC models and ensuring reliable voltage prediction [4], [15]. In recent years, several metaheuristic algorithms have been applied to this problem because of their ability to solve nonlinear, multimodal, and non-differentiable optimization tasks. Nevertheless, many existing studies mainly focus on the best objective-function value, while robustness over independent runs, convergence behavior, computational effort, and the physical relevance of the identified parameters are often less emphasized. These aspects are important for assessing whether an optimization algorithm provides not only accurate curve fitting, but also reliable and reproducible PEMFC model calibration.

To address this issue, this paper investigates the application of the Birds of Prey-Based Optimization (BPBO) algorithm to the parameter identification of PEMFC models. BPBO is a recent population-based metaheuristic inspired by the hunting and prey-tracking behavior of predatory birds [24]. Its search mechanism combines exploration of different regions of the search space with exploitation around promising candidate solutions. This balance makes BPBO suitable for PEMFC parameter estimation, where small changes in semi-empirical parameters may cause significant nonlinear variations in the simulated stack voltage.

The main objective of this work is to minimize the sum of squared errors (SSE) between simulated and experimental stack voltages in order to obtain an accurate set of PEMFC model parameters. The proposed BPBO-based identification framework is validated using two benchmark PEMFC stacks, namely the BCS 500 W and NedStack PS6 systems. The main contributions of this study are: (i) the application of BPBO to constrained PEMFC parameter identification; (ii) the validation of the proposed approach on two benchmark PEMFC stacks; (iii) the evaluation of the fitting accuracy using experimental polarization data; and (iv) the comparison of BPBO with several well-established optimization algorithms in terms of accuracy, robustness, convergence behavior, and computational time.

The remainder of this paper is organized as follows. Section II presents the PEMFC mathematical model and the parameter identification problem. Section III describes the BPBO algorithm and its implementation for PEMFC parameter estimation. Section IV discusses the obtained results and comparative analyses for the considered PEMFC stacks. Finally, Section V concludes the paper and outlines future research directions.

II. PEMFC Modeling

The structure and operating principle of a proton exchange membrane fuel cell (PEMFC) are illustrated in Fig. 1. A PEMFC converts the chemical energy of hydrogen and oxygen directly into electrical energy through electrochemical reactions [9]. It mainly consists of a proton exchange membrane, catalyst layers, gas diffusion layers, and bipolar plates with gas flow channels. At the anode, hydrogen is oxidized into protons and electrons. The protons migrate through the membrane toward the cathode, whereas the electrons flow through the external circuit and generate electrical power. At the cathode, oxygen reacts with the transported protons and electrons to produce water and heat [17].

[1,2,3]University of Tunis, National Higher School of Engineers of Tunis (ENSIT), Laboratory of Engineering of Industrial Systems and Renewable Energy (LISIER), Tunisia. Emails: Gaflotfi@gmail.com, ahmed.jeridi@ensit.u-tunis.tn, abdou.zaaf@ensit.rnu.tn

Nomenclature

Symbol	Description	Symbol	Description
$PEMFC$	Proton Exchange Membrane Fuel Cell	E_{th}	Thermodynamic potential (V)
V_{cell}	Single cell voltage (V)	R_C	Contact resistance (Ω)
N_{cell}	Number of cells	l_m	Membrane thickness (cm)
$\xi_1, \xi_2, \xi_3, \xi_4$	Semi-empirical coefficients	V	Stack voltage (V)
V_{act}	Activation voltage loss (V)	B	Empirical parametric coefficient (Ω·cm)
V_{conc}	Concentration loss voltage (V)	J	Current density (A/cm^2)
J_{max}	Maximum current density (A/cm^2)	λ	Membrane water content
P_H	Hydrogen partial pressure (atm)	P_O	Oxygen partial pressure (atm)
T	Absolute temperature (K)	P_{sat}	Water saturation pressure (atm)
R_{Hu}	Anode vapor relative humidity	R_{He}	Cathode vapor relative humidity
P_a	Anode inlet pressure (atm)	P_c	Cathode inlet pressure (atm)
A	Effective membrane area (cm^2)	G_O	Oxygen concentration (mol/cm^3)

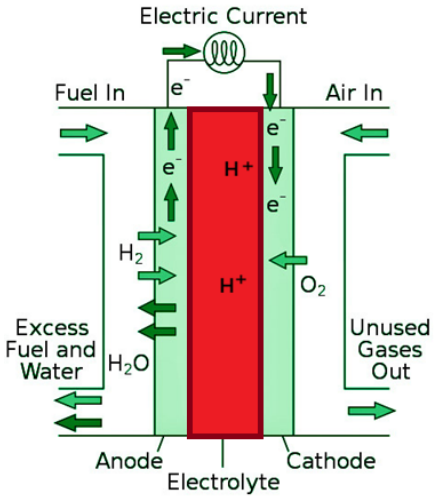

Fig. 1: Schematic structure of a proton exchange membrane fuel cell.

A. Electrochemical Reactions

The electrochemical reactions occurring inside a PEMFC can be expressed as follows. At the anode, hydrogen oxidation is given by

$$2\mathrm{H_2} \rightarrow 4\mathrm{H^+} + 4e^-. \tag{1}$$

At the cathode, oxygen reduction takes place according to

$$\mathrm{O_2} + 4\mathrm{H^+} + 4e^- \rightarrow 2\mathrm{H_2O}. \tag{2}$$

Thus, the overall PEMFC reaction is written as

$$2\mathrm{H_2} + \mathrm{O_2} \rightarrow 2\mathrm{H_2O}. \tag{3}$$

This direct electrochemical conversion process enables PEMFCs to achieve high efficiency and low environmental impact compared with conventional combustion-based energy conversion systems [16].

B. Semi-Empirical Voltage Model

The output voltage of a PEMFC is generally described by its polarization curve, which represents the relationship between voltage and current density [11]. Although the theoretical reversible voltage of the hydrogen–oxygen reaction is approximately 1.229 V under standard conditions, the actual cell voltage is lower due to activation, ohmic, and concentration losses.

The voltage of a single PEMFC cell is expressed as

$$V_{\mathrm{cell}} = E_{\mathrm{Nernst}} - V_{\mathrm{act}} - V_{\mathrm{ohm}} - V_{\mathrm{conc}}, \tag{4}$$

where E_{Nernst} is the reversible thermodynamic voltage, while V_{act}, V_{ohm}, and V_{conc} are the activation, ohmic, and concentration voltage losses, respectively.

For a stack composed of N_{cell} cells connected in series, the stack voltage is given by

$$V_{\mathrm{stack}} = N_{\mathrm{cell}} V_{\mathrm{cell}}. \tag{5}$$

The Nernst voltage is calculated as

$$E_{\mathrm{Nernst}} = 1.229 - 8.5\times10^{-4}(T-298.15) + 4.3085\times10^{-5} T \ln\left(P_{\mathrm{H_2}}\sqrt{P_{\mathrm{O_2}}}\right), \tag{6}$$

where T is the operating temperature in kelvin, and $P_{\mathrm{H_2}}$ and $P_{\mathrm{O_2}}$ are the hydrogen and oxygen partial pressures, respectively.

When air is used as the oxidant, the oxygen partial pressure can be estimated by

$$P_{\mathrm{O_2}} = \frac{P_{\mathrm{c}} - RH_{\mathrm{c}} P_{\mathrm{sat}}}{\left(1 + \frac{79}{21}\right)\exp\left(\frac{269.10}{T^{1.304}}\frac{I}{A}\right)}, \tag{7}$$

where P_{c} is the cathode pressure, RH_{c} is the cathode relative humidity, P_{sat} is the water saturation pressure, I is the operating current, and A is the active membrane area.

The activation voltage loss is associated with the electrochemical reaction kinetics at the electrodes and is modeled as

$$V_{\mathrm{act}} = -\left[\xi_1 + \xi_2 T + \xi_3 T \ln\left(C_{\mathrm{O_2}}\right) + \xi_4 T \ln(I)\right], \tag{8}$$

where ξ_1, ξ_2, ξ_3, and ξ_4 are semi-empirical activation coefficients, and $C_{\mathrm{O_2}}$ is the oxygen concentration at the cathode catalyst interface.

According to Henry's law, the dissolved oxygen concentration is obtained as

$$C_{\mathrm{O_2}} = \frac{P_{\mathrm{O_2}} \exp(498/T)}{5.08 \times 10^6}. \tag{9}$$

The ohmic voltage loss is mainly caused by membrane proton resistance and electrical contact resistance. It is expressed as

$$V_{\mathrm{ohm}} = I\left(R_{\mathrm{m}} + R_{\mathrm{C}}\right), \tag{10}$$

where R_C is the contact resistance and R_m is the membrane resistance. The membrane resistance is defined by

$$R_m = \frac{\rho_m l_m}{A}, \tag{11}$$

where l_m is the membrane thickness and ρ_m is the membrane resistivity.

The membrane resistivity is computed using the following semi-empirical expression [10]:

$$\rho_m = \frac{181.6\left[1 + 0.03J + 0.062\left(\frac{T}{303}\right)^2 J^{2.5}\right]}{[\lambda - 0.634 - 3J]\exp\left[4.18\left(\frac{T-303}{T}\right)\right]}, \tag{12}$$

where $J = I/A$ is the current density and λ is the membrane water content.

The concentration voltage loss is caused by mass-transport limitations, especially at high current densities. It is expressed as

$$V_{conc} = -B\ln\left(1 - \frac{J}{J_{max}}\right), \tag{13}$$

where B is the concentration loss coefficient and J_{max} is the maximum current density.

C. Parameter Identification Problem

The semi-empirical PEMFC model includes several parameters that are difficult to measure directly and must therefore be identified from experimental polarization data. In this study, seven unknown parameters are estimated:

$$\boldsymbol{\theta} = [\xi_1, \xi_2, \xi_3, \xi_4, \lambda, R_C, B]. \tag{14}$$

These parameters have direct physical effects on the PEMFC voltage response. The coefficients ξ_1–ξ_4 mainly influence the activation loss and therefore affect the low-current region of the polarization curve. The membrane water content λ affects membrane conductivity and controls the ohmic loss in the medium-current region. The contact resistance R_C contributes to the total ohmic voltage drop and affects the slope of the polarization curve. The coefficient B governs the concentration loss and becomes more influential near high current densities, where mass-transport limitations are significant. Thus, accurate parameter estimation is important not only for numerical curve fitting, but also for obtaining a physically meaningful PEMFC model.

For a given parameter vector $\boldsymbol{\theta}$, the simulated stack voltage is calculated and compared with the corresponding experimental voltage. The parameter identification problem is formulated as a constrained optimization problem by minimizing the sum of squared errors (SSE):

$$F_{obj}(\boldsymbol{\theta}) = \sum_{i=1}^{N}\left[V_{meas,i} - V_{sim,i}(\boldsymbol{\theta})\right]^2, \tag{15}$$

where N is the number of experimental data points, $V_{meas,i}$ is the measured voltage, and $V_{sim,i}(\boldsymbol{\theta})$ is the simulated voltage at the ith operating point.

The optimal parameter vector is obtained as

$$\boldsymbol{\theta}^* = \arg\min_{\boldsymbol{\theta}\in\Omega} F_{obj}(\boldsymbol{\theta}), \tag{16}$$

where Ω denotes the feasible search space defined by the lower and upper bounds of the identified parameters. In this work, BPBO is used to solve this nonlinear and constrained parameter identification problem.

III. Birds of Prey-Based Optimization

Birds of Prey-Based Optimization (BPBO) is a recent population-based metaheuristic inspired by the hunting, prey-tracking, and attacking behaviors of predatory birds [25]. In BPBO, each candidate solution represents an individual bird, whereas the best solution found so far is considered as the prey. The population evolves iteratively through a combination of prey-guided movements, mean-guided movements, worst-solution avoidance, and random exploratory displacements. These mechanisms allow BPBO to maintain a suitable balance between exploration and exploitation, which is essential for nonlinear and constrained engineering optimization problems.

In this work, BPBO is applied to the PEMFC parameter identification problem, where the objective function is nonlinear and multimodal. Each candidate solution represents a complete vector of unknown PEMFC parameters:

$$X_i = [\xi_1, \xi_2, \xi_3, \xi_4, \lambda, R_C, B]_i. \tag{17}$$

The fitness of each candidate solution is evaluated by the sum of squared errors between measured and simulated stack voltages:

$$f(X_i) = \sum_{k=1}^{N}\left[V_{meas,k} - V_{sim,k}(X_i)\right]^2, \tag{18}$$

where N is the number of experimental data points, $V_{meas,k}$ is the measured voltage, and $V_{sim,k}(X_i)$ is the simulated voltage obtained using the parameter vector X_i.

Let X_{best}, X_{worst}, and X_{mean} denote the best solution, the worst solution, and the mean position of the population, respectively. The population mean is calculated as

$$X_{mean} = \frac{1}{N_{pop}}\sum_{i=1}^{N_{pop}} X_i, \tag{19}$$

where N_{pop} is the population size.

During the exploitation phase, candidate solutions are updated toward promising regions using the following operators:

$$X_i^{new} = X_i + r\left(X_{best} - MX_i\right), \tag{20}$$

$$X_i^{new} = X_{mean} + r\left(X_{best} - MX_{mean}\right), \tag{21}$$

$$X_i^{new} = X_i + r\left(X_i - MX_{worst}\right), \tag{22}$$

where r is a random number uniformly distributed in $[0, 1]$, and M is a random integer selected from $\{1, 2\}$. Equations (20) and (21) intensify the search around promising regions, while (22) helps move candidate solutions away from poor regions of the search space.

In the exploration phase, a random displacement is introduced as

$$X_i^{new} = X_i + r\,U(LB, UB), \tag{23}$$

where LB and UB are the lower and upper parameter bounds, respectively, and $U(LB, UB)$ is a random vector generated within the feasible range. After each update, boundary control is applied as

$$X_{i,j}^{new} = \min\left[\max\left(X_{i,j}^{new}, LB_j\right), UB_j\right], \qquad j = 1, \ldots, D, \tag{24}$$

where $D = 7$ is the number of identified PEMFC parameters.

The main steps of the BPBO-based PEMFC parameter identification procedure are summarized in Algorithm 1. The corresponding flowchart is shown in Fig. 2.

The computational cost of BPBO mainly depends on the number of iterations, the population size, and the number of experimental points used in the objective function. Therefore,

Algorithm 1 BPBO-based PEMFC parameter identification

Require: Experimental data, PEMFC model, LB, UB, N_{pop}, $T_{\max}$, switching probability P_s
Ensure: Best parameter vector X_{best} and minimum SSE f_{best}
Initialize the population X_i, $i = 1, \ldots, N_{\text{pop}}$, within $[LB, UB]$
Evaluate the fitness $f(X_i)$ of each candidate solution
Determine X_{best} and X_{worst}
for $t = 1$ to $T_{\max}$ **do**
  Compute X_{mean} using (19)
  Update X_{best} and X_{worst}
  for $i = 1$ to N_{pop} **do**
    Generate random numbers $r_1, r_2, r_3 \in [0, 1]$
    Generate a random integer $M \in \{1, 2\}$
    if $r_1 < P_s$ **then**
      if $r_2 < 1/3$ **then**
        Generate X_i^{new} using (20)
      else if $r_2 < 2/3$ **then**
        Generate X_i^{new} using (21)
      else
        Generate X_i^{new} using (22)
      end if
    else
      Generate X_i^{new} using (23)
    end if
    Apply boundary control using (24)
    Evaluate $f(X_i^{new})$
    if $f(X_i^{new}) < f(X_i)$ **then**
      Replace X_i with X_i^{new}
    end if
    if $f(X_i) < f(X_{\text{best}})$ **then**
      Update $X_{\text{best}} = X_i$
    end if
  end for
  Store the best SSE value at iteration t
end for
return X_{best} and f_{best}

TABLE I: Operating conditions of the studied PEMFC stacks.

Stack	N_{cell}	A (cm^2)	l_{m} (μm)	T (K)	P_{H_2} (atm)	P_{O_2} (atm)	$J_{\max}$ (A/cm^2)
NedStack PS6	64	242	175	343	1	1	5.00000
BCS 500 W	32	62	175	333	1	1	0.52922

the approximate complexity of the proposed BPBO-based identification procedure is

$$\mathcal{O}\left(T_{\max} N_{\text{pop}} N\right). \tag{25}$$

Since only seven PEMFC parameters are optimized, this complexity remains acceptable. Moreover, the use of both exploitation and exploration operators allows BPBO to refine accurate solutions while reducing the risk of premature convergence. This makes the proposed method suitable for constrained PEMFC model calibration.

IV. Results and Discussion

All optimisation routines were implemented in MATLAB R2024a on a workstation equipped with an Intel® Core™ i7 CPU and 16 GB of RAM. For the benchmark functions, a population size of $N = 30$ and a maximum of $T_{\max} = 500$ iterations were adopted, resulting in an identical number of objective-function evaluations for all methods. To account for stochasticity, each configuration was repeated 30 times using different random seeds. The random number generator was initialised via `rng(2024)` for the first run and incremented by one for each subsequent run. The raw I–V datasets for BCS 500 W and Nedstack PS6, together with the MATLAB source codes used for objective-function evaluation and optimisation, are provided as supplementary material to ensure the exact reproducibility of the reported results.

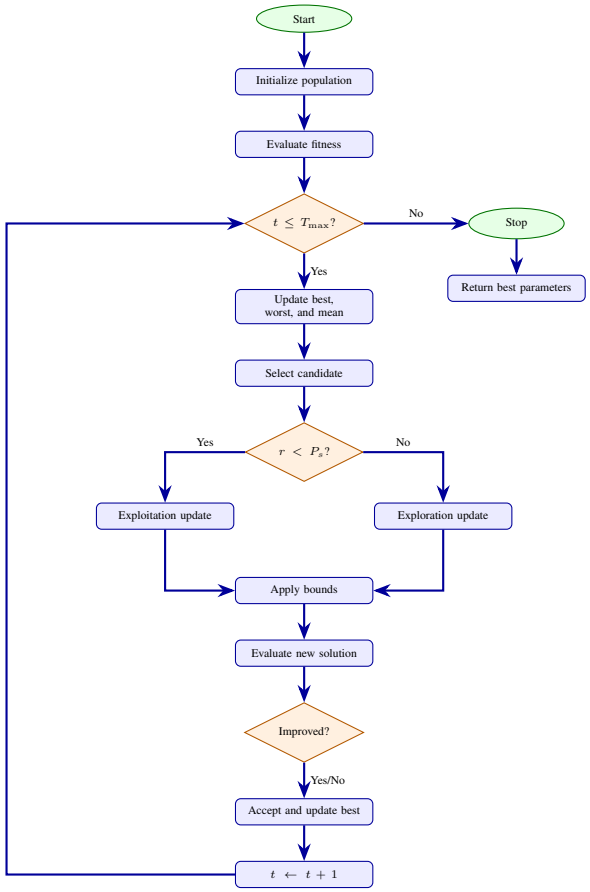

Fig. 2: Compact flowchart of the BPBO-based PEMFC parameter identification procedure.

TABLE II: Search-space bounds of the identified PEMFC parameters.

Bound	ξ_1	ξ_2	ξ_3	ξ_4	λ	R_C	B
Lower	-1.19669	1.0×10^{-3}	3.6×10^{-5}	-2.6×10^{-4}	10	1.0×10^{-4}	0.136
Upper	-0.8532	5.0×10^{-3}	9.8×10^{-5}	-9.54×10^{-5}	24	8.0×10^{-4}	0.5

For the PEMFC case studies, all algorithms were executed under a unified identification protocol in order to ensure fair comparisons. Unless otherwise stated, a common population size of $N = 50$ and a common maximum number of iterations $T_{\max}$ were used for every optimiser, thereby fixing the total computational budget in terms of objective-function evaluations across all methods. The seven unknown model parameters were estimated within dataset-agnostic yet physically plausible bounds, as reported in Table II. These intervals were selected by combining representative ranges reported in PEMFC parameter-estimation studies [18], [19], [20], [21], [25] with basic physical constraints, such as non-negative resistances and realistic activation coefficients. In particular, the membrane water content $\lambda \in [10, 24]$ covers the standard hydration range of Nafion-type membranes under the operating conditions considered. The operating conditions associated with each fuel-cell stack are summarised in Table I.

A. Parameter Identification Setup

The PEMFC model considered in this study involves seven unknown parameters that must be accurately identified in order to ensure reliable voltage prediction. The corresponding

search intervals are reported in Table II, whereas the operating conditions of the investigated fuel-cell stacks are summarised in Table I.

The parameter-identification task was carried out using the proposed BPBO algorithm. The optimisation procedure was implemented in MATLAB and executed on an Intel Core i5 platform. In order to assess the effectiveness of BPBO, its performance was compared with several well-established optimisation algorithms available in the literature, namely ICA, SFLA, SSO, ISCE, FOA, NNA, GWO, and HHO. For a fair comparison, all competing methods were tested under the same computational settings, namely a population size of 50 and a maximum of 1000 objective-function evaluations.

The obtained results demonstrate that BPBO ensures stable convergence and high estimation accuracy, thereby confirming its suitability for PEMFC parameter identification.

B. Results for the Nedstack PS6 Fuel Cell

Figure 3 presents the experimental and simulated polarisation characteristics of the Nedstack PS6 fuel cell. More specifically, Figure 3a shows the I–V polarisation curve, whereas Figure 3b depicts the corresponding I–P curve. In both cases, a close agreement between the simulated and experimental profiles can be observed, confirming the accuracy of the identified parameter set and the capability of the proposed model to reproduce the nonlinear behaviour of the PEMFC system.

The optimisation performance of BPBO for the Nedstack PS6 case is illustrated in Figure 4. Figure 4a compares the convergence behaviour of BPBO with that of the competing methods, showing that BPBO reaches a lower objective-function value more rapidly. In addition, Figure 4b provides an RMSE-based statistical comparison, from which BPBO can be seen to exhibit both competitive accuracy and stable performance.

The numerical results reported in Table ?? further confirm these observations. For the Nedstack PS6 fuel cell, BPBO achieves the lowest SSE value among all compared algorithms, equal to 2.06556, thereby demonstrating its effectiveness for this benchmark problem.

C. Results for the BCS 500 W Fuel Cell

Figure 5 presents the experimental and simulated polarisation characteristics of the BCS 500 W fuel cell. Figure 5a illustrates the I–V polarisation curve, whereas Figure 5b shows the corresponding I–P curve. The close agreement between the simulated and experimental results confirms the reliability of the identified parameters and the predictive capability of the adopted PEMFC model.

The optimisation performance for this test case is summarised in Figure 6. As shown in Figure 6a, BPBO converges rapidly towards a low objective-function value and exhibits a stable convergence trend compared with the other methods. Furthermore, the RMSE-based statistical comparison in Figure 6b indicates that BPBO achieves accurate and robust estimation performance.

According to Table ??, BPBO attains an SSE value of 0.011697 for the BCS 500 W system, placing it among the best-performing methods considered in this study and confirming the effectiveness of the proposed approach for PEMFC parameter estimation.

D. Comparative Assessment

To further evaluate the performance of BPBO, a comparative analysis was conducted against several optimisation algorithms reported in the literature. The comparison was based on the sum of squared errors (SSE) between the estimated and experimental voltage values, where a lower SSE indicates better fitting accuracy.

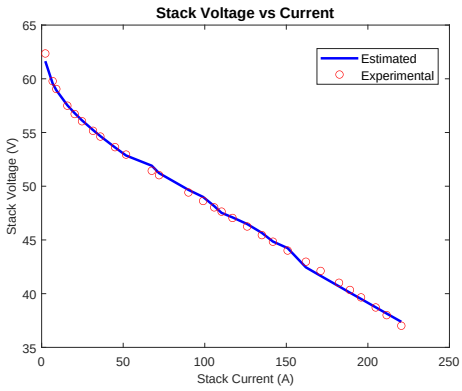

(a) I–V polarisation curve.

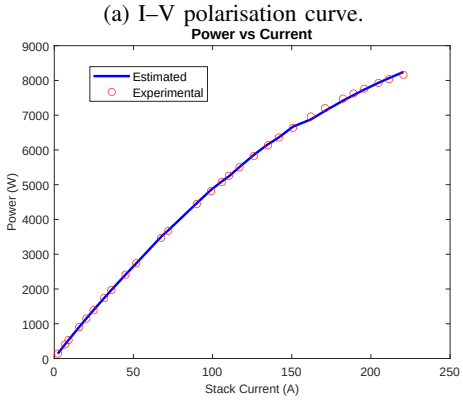

(b) I–P polarisation curve.

Fig. 3: Experimental and simulated polarisation characteristics of the Nedstack PS6 fuel cell.

The comparative results listed in Table ?? show that BPBO provides highly competitive performance for both PEMFC benchmark cases considered in this work. In particular, BPBO achieves the best result for the Nedstack PS6 fuel cell, with the lowest SSE value among all tested methods. For the BCS 500 W fuel cell, BPBO also exhibits very strong performance and remains among the most accurate methods included in the comparison.

Overall, the obtained results confirm that BPBO is an accurate, robust, and reliable optimisation approach for PEMFC parameter identification. Its ability to provide precise voltage estimation and favourable convergence behaviour under different operating conditions makes it a promising tool for fuel-cell modelling and performance analysis.

E. Comparison with Other Algorithms

To further assess the performance of BPBO, a comparative analysis was conducted against several optimisation methods available in the literature. The comparison was based on the sum of squared errors (SSE) between the estimated and experimental voltage values, where a smaller SSE indicates a better fit to the experimental data.

Figure 7 shows the polarisation curves corresponding to the Horizon 500 W PEMFC under two different operating conditions: a pressure of 3/5 bar at a temperature of 353.15 K, and a pressure of 1/1 bar at a temperature of 343.15 K. The comparison between the experimental and modelled voltages reveals only slight deviations over the entire operating range. These discrepancies can mainly be attributed to the variation of two sensitive parameters, namely the equivalent membrane resistance (R_m) and the maximum current density ($J_{\max}$). Since

TABLE III: Comparative parameter identification results for the studied PEMFC stacks.

Algorithm	ξ_1	ξ_2 (10^{-3})	ξ_3 (10^{-5})	ξ_4 (10^{-5})	λ	R_C (10^{-4})	B (10^{-2})	SSE
BCS 500 W								
BPBO	−1.07573	3.57934	8.10216	−1.93018	20.87742	1.0010	0.01613	**0.011697**
GWO [4]	−1.01830	2.31510	5.24000	−1.28150	18.85470	0.7504	0.01136	7.18890
SSO [4]	−1.01800	2.31510	5.24000	−1.28150	18.85470	7.5036	0.01360	7.18890
ICA [17]	−0.90860	2.47980	4.45830	−19.3400	22.66700	2.4630	1.62500	0.01185
SFLA [17]	−0.96574	3.08000	7.22360	−19.3010	20.88620	1.0000	1.61260	0.01160
HHO	−1.02030	2.32020	5.24060	−1.28100	18.85400	0.7330	0.01000	7.19102
FOA [17]	−0.99280	2.62100	3.74636	−19.3600	21.10100	1.0000	1.62690	0.01180
Nedstack PS6								
BPBO	−0.85313	2.39873	3.60020	−9.54020	12.57434	0.1000	0.01360	**2.06556**
GWO [4]	−1.07823	3.38556	5.96780	−9.54010	12.57000	0.1000	0.01360	2.07917
ICA [4]	−1.03432	3.32020	6.44208	−9.54020	15.09700	1.6500	1.36000	2.16830
HHO	−0.85320	3.34876	9.36010	−9.54030	13.07090	0.1000	0.01360	2.09068
NNA [18]	−0.85350	2.43160	3.75450	−9.54010	13.08300	0.1000	1.36000	2.14480
SFLA [4]	−1.02307	3.47600	7.78833	−9.54080	15.03229	1.6200	1.36000	2.16706
FOA [4]	−1.03566	2.95020	3.76690	−9.54000	15.02900	1.6220	1.36000	2.16709
SSO [4]	−0.97190	3.34870	7.91110	−9.54350	13.00000	1.0000	5.34000	2.18067

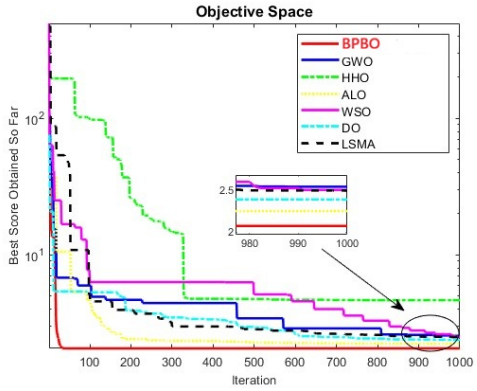

(a) Convergence curves of BPBO and the compared algorithms.

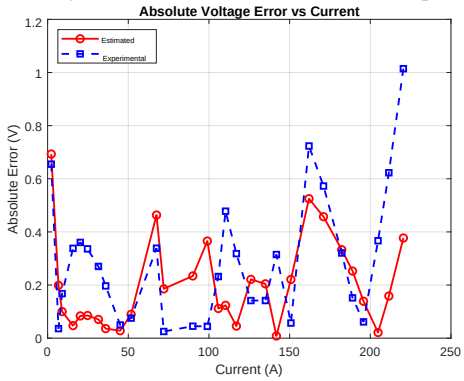

(b) RMSE-based statistical comparison.

Fig. 4: Optimisation performance of BPBO for the Nedstack PS6 fuel cell.

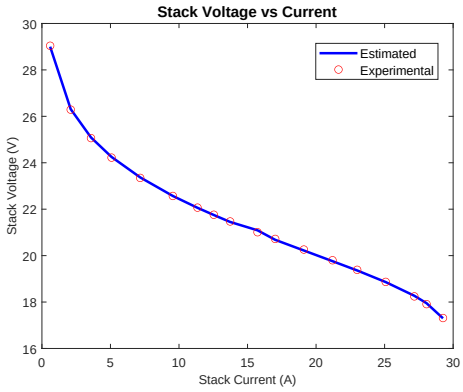

(a) I–V polarisation curve.

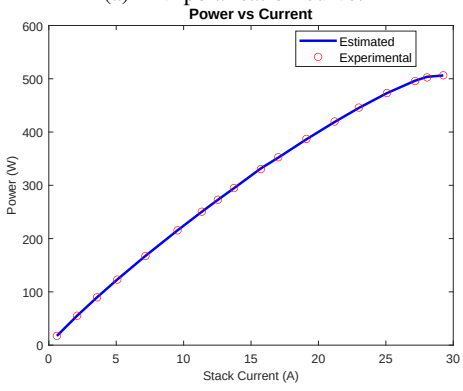

(b) I–P polarisation curve.

Fig. 5: Experimental and simulated polarisation characteristics of the BCS 500 W fuel cell.

both quantities are affected by temperature and pressure, their variation directly influences the prediction accuracy of the theoretical model.

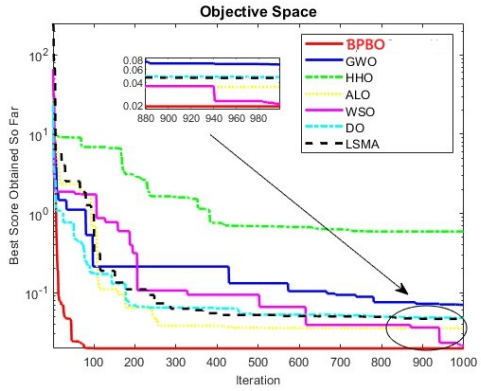

(a) Convergence curves of BPBO and the compared algorithms.

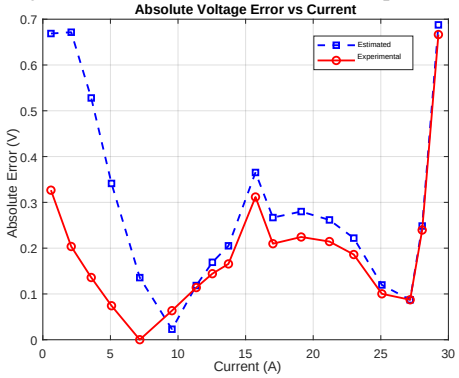

(b) RMSE-based statistical comparison.

Fig. 6: Optimisation performance of BPBO for the BCS 500 W fuel cell.

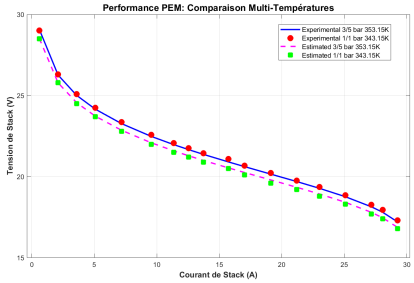

Fig. 7: Polarisation curves for the Horizon 500 W PEMFC under different temperature and pressure conditions.

The comparative results in Table ?? show that BPBO delivers highly competitive performance for the considered PEMFC parameter-estimation problems. In particular, it achieves the best result for the Nedstack PS6 case and maintains very strong performance for the other reported case, with SSE values that remain among the lowest in the comparison.

Overall, the obtained results confirm that BPBO is an accurate, robust, and reliable optimisation method for PEMFC parameter identification. Its ability to provide precise voltage estimation under different operating conditions makes it a promising approach for fuel-cell modelling and performance analysis.

Table IV presents the statistical performance of BPBO and the compared algorithms for the BCS 0.5 kW and Nedstack PS6 PEMFC cases in terms of minimum, mean, and maximum SSE, standard deviation, and elapsed time. For the BCS 500 W case,

TABLE IV: Statistical performance of BPBO and the compared algorithms.

Algorithm	Min	Mean	Max	Std.	Time (s)
BCS 500 W					
BPBO	**0.011697**	**0.011727**	**0.011796**	**3.65E−05**	**23.67**
GWO	0.011744	0.014062	0.020112	$2.72E-03$	111.75
SSO	0.011950	0.016711	0.021699	$4.30E-03$	237.13
HHO	0.012095	0.012820	0.014914	$9.30E-04$	95.80
FOA	0.011781	0.012891	0.015595	$1.49E-03$	338.54
Nedstack PS6					
BPBO	**2.065560**	**2.135662**	**2.329817**	$6.96E-02$	**35.46**
GWO	2.110850	2.321838	2.914057	$2.55E-01$	179.91
SSO	2.416243	2.460612	2.495732	**3.00E−02**	523.26
HHO	2.169365	2.351896	2.682705	$1.75E-01$	159.71
FOA	2.138593	2.382487	2.677051	$1.76E-01$	293.78

BPBO achieves the best performance across all reported indices, including the lowest mean SSE and the shortest execution time, confirming its high estimation accuracy and computational efficiency. For the Nedstack PS6 case, BPBO again yields the best minimum, mean, and maximum SSE values, as well as the lowest elapsed time, whereas SSO attains the smallest standard deviation. Overall, these results demonstrate that BPBO provides a highly competitive balance between estimation accuracy, robustness, and computational cost.

V. Conclusion

This paper addressed the parameter identification problem of proton exchange membrane fuel cell (PEMFC) models using the Birds of Prey-Based Optimization (BPBO) algorithm. The proposed approach was applied to two benchmark PEMFC systems, namely the Nedstack PS6 and BCS 500 W fuel cells, with the objective of minimizing the sum of squared errors (SSE) between the simulated and experimental voltage data.

The obtained results demonstrate that BPBO can provide accurate parameter estimates and favorable convergence behavior for both PEMFC cases considered. In particular, the proposed method achieved the best performance for the Nedstack PS6 fuel cell and remained highly competitive for the BCS 500 W system when compared with several well-established optimization algorithms reported in the literature. These findings confirm that BPBO represents a robust and effective optimization framework for PEMFC parameter identification.

Overall, this study highlights the potential of BPBO as a reliable tool for improving PEMFC model calibration and voltage prediction accuracy. Future work may focus on extending the proposed framework to dynamic PEMFC models, multi-objective formulations, and hybrid data-driven modeling strategies to further enhance prediction capability and practical applicability under real operating conditions.

References

[1] Veziroglu, A., & Macario, R. (2011). Fuel cell vehicles: Current advancements with economic and ecological considerations. *International Journal of Hydrogen Energy*, 36(1), 25–43. https://doi.org/10.1016/j.ijhydene.2010.08.145

[2] Priya, K., Sathishkumar, K., & Rajasekar, N. (2018). A thorough examination of parameter estimation methods for modeling proton exchange membrane fuel cells. *Renewable and Sustainable Energy Reviews*, 93, 121–144. https://doi.org/10.1016/j.rser.2018.05.017

[3] Kandidayeni, M., Macias, A., Amamou, A. A., Boulon, L., Kelouwani, S., & Chaoui, H. (2018). A survey and comparative analysis of fuel cell parameter estimation techniques for energy management applications. *Journal of Power Sources*, 380, 92–104. https://doi.org/10.1016/j.jpowsour.2018.01.075

[4] Ozdemir, M. T. (2021). Enhanced parameter estimation for polymer electrolyte membrane fuel cell models using chaos-integrated particle swarm optimization. *International Journal of Hydrogen Energy*, 46(30), 16465–16480. https://doi.org/10.1016/j.ijhydene.2020.12.203

[5] Li, J., Gao, X., Cui, Y., Hu, J., Xu, G., & Zhang, Z. (2020). Reliable, accurate, and efficient parameter extraction for PEM fuel cells using a shuffled multi-simplexes search method. *Energy Conversion and Management*, 206, 112501. https://doi.org/10.1016/j.enconman.2020.112501

[6] Miao, D., Chen, W., Zhao, W., & Demsas, T. (2020). Parameter estimation of PEM fuel cells using a hybrid grey wolf optimization technique. *Energy*, 193, 116616. https://doi.org/10.1016/j.energy.2019.116616

[7] Heidari, A. A., Mirjalili, S., Faris, H., Aljarah, I., Mafarja, M., & Chen, H. (2019). Harris hawks optimization: Algorithm design and its applications. *Future Generation Computer Systems*, 97, 849–872. https://doi.org/10.1016/j.future.2019.02.028

[8] Shehab, M., Mashal, I., Momani, Z., Shambour, M. K. Y., AL-Badareen, A., Al-Dabet, S., & Alomari, O. A. (2022). Harris hawks optimization algorithm: Variants and applications. *Archives of Computational Methods in Engineering*, 29(7), 5579–5603. https://doi.org/10.1007/s11831-022-09780-1

[9] Calasan, M., Abdel Aleem, S. H. E., Hasanien, H. M., Alaas, Z. M., & Ali, Z. M. (2023). An innovative approach for mathematical modeling and parameter estimation of PEM fuel cells based on iterative Lambert W function. *Energy*, 264, 126165. https://doi.org/10.1016/j.energy.2022.126165

[10] Li, Y., Yang, F., Chen, D., Hu, S., & Xu, X. (2023). A thermal-physical modeling and parameter identification approach for a dynamic model with unobservable states in a 10-kW PEM fuel cell system. *Energy Conversion and Management*, 276, 116580. https://doi.org/10.1016/j.enconman.2022.116580

[11] Mirjalili, S., Mirjalili, S. M., & Lewis, A. (2014). Grey wolf optimizer: An innovative approach. *Advances in Engineering Software*, 69, 46–61. https://doi.org/10.1016/j.advengsoft.2013.12.007

[12] Makhadmeh, S. N., Al-Betar, M. A., Doush, I. A., Awadallah, M. A., Kassaymeh, S., Mirjalili, S., & Zitar, R. A. (2024). Recent advances in Grey Wolf Optimizer, its versions and applications: Review. *IEEE Access*, 12, 22991–23028. https://doi.org/10.1109/ACCESS.2023.3304889

[13] Tummala, A. S. L. V., Polumahanthi, N., Khan, B., & Ali, A. (2024). Accurate parameters identification of proton exchange membrane fuel cell using Young's double-slit experiment optimizer. *Frontiers in Energy Research*, 12, 1384649. https://doi.org/10.3389/fenrg.2024.1384649

[14] Pan, M., Pan, C., Li, C., & Zhao, J. (2021). A review of membranes in proton exchange membrane fuel cells: Transport phenomena, performance and durability. *Renewable and Sustainable Energy Reviews*, 141, 110771. https://doi.org/10.1016/j.rser.2021.110771

[15] Ayyarao, T. S. L. V., Polumahanthi, N., & Khan, B. (2024). An accurate parameter estimation of PEM fuel cell using war strategy optimization. *Energy*, 290, 130235. https://doi.org/10.1016/j.energy.2024.130235

[16] Zhou, Y., Wang, B., Ling, Z., Liu, Q., Fu, X., Zhang, Y., Zhang, R., Hu, S., Zhao, F., Li, X., Bao, X., & Yang, J. (2024). Advances in ionogels for proton-exchange membranes. *Science of the Total Environment*, 921, 171099. https://doi.org/10.1016/j.scitotenv.2024.171099

[17] Kandidayeni, M., Macias, A., Khalatbarisoltani, A., Boulon, L., & Kelouwani, S. (2019). Benchmark of proton exchange membrane fuel cell parameters extraction with metaheuristic optimization algorithms. *Energy*, 183, 912–925. https://doi.org/10.1016/j.energy.2019.06.152

[18] Fawzi, M., El-Fergany, A. A., & Hasanien, H. M. (2019). Effective methodology based on neural network optimizer for extracting model parameters of PEM fuel cells. *International Journal of Energy Research*, 43(14), 8136–8147. https://doi.org/10.1002/er.4809

[19] Abdel-Basset, M., Mohamed, R., Elhoseny, M., Chakrabortty, R. K., & Ryan, M. J. (2021). An efficient heap-based optimization algorithm for parameters identification of proton exchange membrane fuel cells model: Analysis and case studies. *International Journal of Hydrogen Energy*, 46(21), 11908–11925. https://doi.org/10.1016/j.ijhydene.2021.01.076

[20] Rezk, H., Olabi, A. G., Ferahtia, S., & Sayed, E. T. (2022). Accurate parameter estimation methodology applied to model proton exchange membrane fuel cell. *Energy*, 255, 124454. https://doi.org/10.1016/j.energy.2022.124454

[21] Gao, X., et al. (2018). Parameter extraction for solar cell models using an enhanced shuffled complex evolution algorithm. *Energy Conversion and Management*, 157, 460–479. https://doi.org/10.1016/j.enconman.2017.12.033

[22] Jeridi, A., Moulahi, M. H., Khaterchi, H., et al. (2024). A hybrid method integrating WSO-HO and Newton-Raphson for optimizing photovoltaic solar model parameters. *Power Electronics and Drives*, 10. https://doi.org/10.2478/pead-2025-0003

[23] Jeridi, A., Moulahi, M. H., Messaoud, R. B., et al. (2024). Improving photovoltaic solar model parameter optimization with a WSO-MTBO hybrid method based on Newton-Raphson. *Przeglad Elektrotechniczny*, 11, 133–140. https://doi.org/10.15199/48.2024.11.25

[24] Ghasemi, M., Akbari, M. A., Zare, M., Mirjalili, S., Deriche, M., Abualigah, L., & Khodadadi, N. (2025). Birds of prey-based optimization (BPBO): A metaheuristic algorithm for optimization. *Evolutionary Intelligence*, 18, Article 88. https://doi.org/10.1007/s12065-025-01052-8

[25] Jeridi, A., et al. (2026). Hybrid metaheuristic optimization for accurate PEM fuel cell parameter estimation: Combining grey wolf optimizer and Harris hawks optimization. *Engineering Research Express*.

[26] Jeridi A, Moulahi MH, Khaterchi H, Zaafouri A. An improved gorilla troops optimizer for enhanced parameter estimation of proton exchange membrane fuel cells. *World Journal of Engineering*. 2026;1–20. doi:10.1108/WJE-10-2025-0670.